Carbon nanotubes induce inflammation but decrease the production of reactive oxygen species in lung

D. Crouzier[a,*], S. Follot[a], E. Gentilhomme[b], E. Flahaut[c,d], R. Arnaud[a], V. Dabouis[a], C. Castellarin[b], J.C. Debouzy[a]

[a] *Unité BCM, Institut de Recherches Biomédicale des Armées/Antenne CRSSA, 24, avenue des maquis du Grésivaudan, BP 87-38 702 La Tronche Cedex, France*
[b] *Service de microscopie et d'imagerie, Institut de Recherches Biomédicale des Armées/Antenne CRSSA, 24, avenue des maquis du Grésivaudan, BP 87-38 702 La Tronche Cedex, France*
[c] *Université de Toulouse, UPS, INP, Institut Carnot Cirimat, 118, route de Narbonne, F-31062 Toulouse cedex 9, France*
[d] *CNRS, Institut Carnot Cirimat, F-31062 Toulouse, France*

A B S T R A C T

With the rapid spread of carbon nanotubes (CNTs) applications, the respiratory toxicity of these compounds has attracted the attention of many scientists. Several studies have reported that after lung administration, CNTs could induce granuloma, fibrosis, or inflammation. By comparison with the mechanisms involved with other toxic particles such as asbestos, this effect could be attributed to an increase of oxidative stress. The aim of the present work was to test this hypothesis *in vivo*.

Mice were intranasally instilled with 1.5 mg/kg of double walled carbon nanotubes (DWCNTs). Six, 24, or 48 h after administration, inflammation and localisation of DWCNTs in lungs were microscopically observed. Local oxidative perturbations were investigated using ESR spin trapping experiments, and systemic inflammation was assessed by measuring the plasma concentration of cytokines TNF-α, IL-1α, IL-1β, IL-6, IGF-1, Leptin, G-CSF, and VEGF.

Examination of lungs and the elevation of proinflammatory cytokines in the plasma (Leptin and IL-6 at 6 h) confirmed the induction of an inflammatory reaction. This inflammatory reaction was accompanied by a decrease in the local oxidative stress. This effect could be attributed to the scavenger capability of pure CNTs.

Keywords:
Double walled carbon nanotubes
Inflammatory reaction
Leptin
Lung
ROS
Spin trap

1. Introduction

Carbon nanotubes (CNTs), allotropes of carbon from the fullerene family, have many interesting and specific mechanical (one of the best strength/weight ratio), electrical (conductors or semiconductors depending on the chiral vector describing their structure) or thermal properties (good thermal conductors along the longitudinal axis). These features make them very useful in many industrial applications such as electronics, optics, aeronautics and are now considered as an interesting field of research for biological application (e.g., vessel for drug delivery, or MRI contrast agents).

Due to their morphological similarity with asbestos fibres, the question of possible potential health hazard arose to become a major concern in public health; this is particularly true for workers and professional users, especially if one considers the increasing and wide spreading of CNTs applications. Hence, CNTs have small size (micrometer range), high aspect ratio (length-to-diameter ratio up to 28,000,000:1) (Park et al., 2009) which means a fibre-like structure, according to the WHO (World Health Organisation) definition, and a high specific surface area (up to 1000 m^2/g) (Peigney et al., 2001). As a consequence, CNTs are extremely aerosolized, making respiratory contamination by inhalation rather likely to occur. In order to determinate the consequences of CNTs inhalation, the first step was to identify the various factors involved in possible toxicity of CNTs. The determine of the toxicity of inhaled particles involves three main factors (Fenoglio et al., 2006) acting together: the shape of the particle (fibre-like or spherical), the surface reactivity (potential to generate free radicals) and its clearance from the respiratory tract. From such criteria, CNTs appeared as potentially highly harmful particles. More recent studies concluded that CNTs would induce mesothelioma or cancer of the lining of the lung, similar tos asbestos fibres (Poland et al., 2008). Other studies reported that purified multi walled carbon nanotubes (MWCNTs) as well as single walled carbon nanotubes (SWCNTs) could result in both inflammatory and fibrotic reactions (Lam et al., 2004; Muller

* Corresponding author at: Centre de Recherche du Service de Santé des Armées, 24, Avenue des maquis du Grésivaudan, BP 87, 38702 La Tronche Cedex, France. Tel.: +33 4 76 63 69 39; fax: +33 4 76 63 69 22.
E-mail address: david.crouzier@wanadoo.fr (D. Crouzier).

doi:10.1016/j.tox.2010.04.001

et al., 2005). When directly administered in the trachea, a stimulation of the production of TNF-α, and also the formation of alveolitis and collagen-rich granuloma were reported (Muller et al., 2005). Such reactions have been observed with asbestos fibres or silica dust and were ascribed to the generation of reactive oxygen species (ROS) (Castranova, 2004; Kamp et al., 1992). It is well established that the ROS released by phagocyting cells react with extracellular fluids (Brown et al., 2000; Fenoglio et al., 2000), cellular products (Crouzier et al., 2009) or directly damage target cells (Kane, 1996; Stadtman, 1990). Some authors also reported that CNT-induced inflammation would be characterized by alveolar cell count increase (neutrophils, eosinophils and macrophages) (Muller et al., 2005; Shvedova et al., 2005).

However, numerous other studies failed to exhibit any toxicological effect, while no ROS production was detected when macrophage cells were stimulated with purified SWCNTs (Shvedova et al., 2005), or no alteration in cell viability or on metabolism in human umbilical vein endothelial cells was observed (Flahaut et al., 2006). Finally, the controversy in evaluating the toxicity on such heterogeneous material still subsists: for instance the parameters such as structure, agglomeration and purity of the sample have considerable impact on the reactivity of CNTs.

These features led us to assess inflammation induction and ROS production after exposure to double walled carbon nanotubes (DWCNTs) by using mice as *in vivo* model. The ROS production in lungs was assayed by recording ESR spin trapping experiments after 6, 24 and 48 h following DWCNTs intranasal administration. The systemic proinflammatory response was simultaneously estimated by measuring the serum concentration of the cytokines TNF-α, IL-1α, IL-1β, IL-6, IGF-1, Leptin, G-CSF, and VEGF. A specific attention was focused on the Leptin which appears as more specifically involved during lungs inflammation (Broekhuizen et al., 2005a) and lungs cancer (Karapanagiotou et al., 2008). Besides, the lungs were microscopically examined to evidence cellular changes, inflammation and the CNTs distribution homogeneity.

2. Materials and methods

2.1. Animals

All procedures were in accordance with the standards for animal care established by Army Biomedical Research Institute (IRBA) and were approved by IRBA ethic committee for animal experimentations (decree 87-848 19 October 1987 edited by the French government).

40 male Swiss mice (Elevage Charles River, France) weighting 30–35 g were used, and were housed ten per cage at control temperature (24 °C) with 12 h/12 h light-dark cycle (dark period from 6 p.m. to 6 a.m.). Food and water were available ad libitum.

2.2. Synthesis and characterization of CNTs

DWCNTs were produced by CCVD decomposition of CH_4 over $Mg_{1-x}Co_xO$ solid solution containing small addition of molybdenum. After the CCVD, the catalyst and by products were removed by treatment of the sample with a concentrated aqueous HCl solution. High-resolution transmission electron microscopy showed that a typical sample consists of *ca.* 80% DWCNTs, 20% Single walled nanotubes, and a few triple-walled carbon nanotubes. The diameter distribution of the DWCNTs ranged from 0.5 to 2.5 nm for inner tubes and from 1.2 to 3.2 nm for outer tubes. The length of individual DWCNTs usually ranges between 1 and 10 μm, although bundles may be much longer (up to 100 μm at least). Due to the synthesis and catalyst-elimination process, the walls of the DWCNTs are not expected to be functionalized (and in particular not by oxygen-containing functional groups).

2.3. CNTs Intranasal instillation

DWCNTs were homogenised in saline. To ensure the whole dispersion of large aggregates, the suspension was sonicated during 30 min. Mice were lightly anaesthetized using isofluorane. DWCNTs were delivered by intranasal instillation at dose of 1.5 mg/kg in a total volume of 50 μl per mouse. The animals were sacrified at 6 h, 24 h and 48 h after treatment. Control group received a saline instillation. A positive control group was made using intranasal instillation of bleomycin at 1.5 mg/kg, which is well known to induce ROS production in lungs (Sato et al., 2008). Animals of this group were sacrified 6 h after treatment.

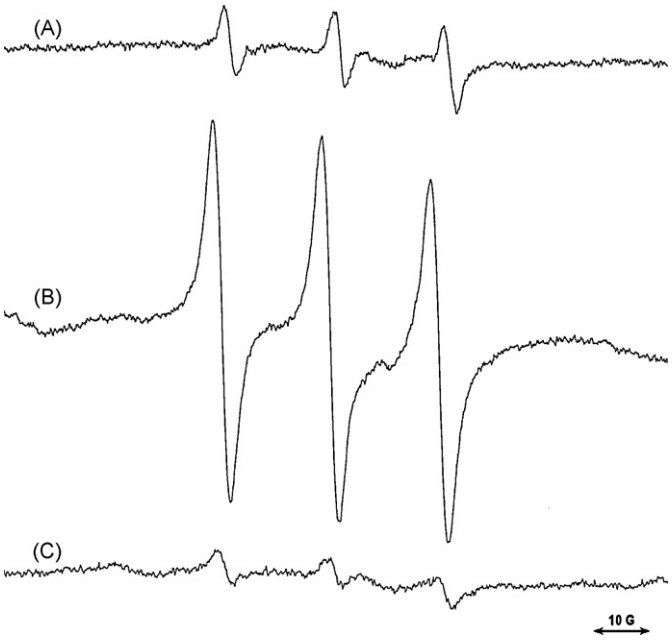

Fig. 1. *In vivo* detection of radical adducts. Electron paramagnetic resonance spectra of N-tert-butyl-α-(4-pyridyl)nitrone N'oxide (4-POBN) radical adducts in lipid extract of mice lung. (A) Spectrum from lung of control mice with saline intranasal instillation, (B) spectrum from positive control mice 6 h after bleomycin instillation, and (C) spectrum from 6 h DWCNTs exposed mice 6 h after DWCNTs instillation.

2.4. In vivo ESR spin trapping studies

One hour before selected time (i.e., 5, 23, and 47 h after CNTs instillation), mice were anesthetized with pentobarbital (30 mg/kg) and were injected intraperitoneally with the spin trap α-(4-pyridyl-1-oxide)-N-t-butylnitrone (4-POBN, Sigma, France) at 4 mmol/kg. To minimize the dehydration effect related with pentobarbital and spin trap injection, 500 μl of saline and atropine at 0.3 mg/kg were also subcutaneously injected.

The animals were sacrificed 1 h after 4-POBN injection, and 800 μl of blood were punctured from intracardiac cavities for the inflammatory response assessment. The lungs were removed, middle lobe of the right lung was used for histopathological analysis while a lipid extract was performed on remaining lungs tissues for radical adduct measurement. These procedures were performed at 4 °C to limit the radical adduct degradation. The tissues were homogenised in 2.5 ml of 2:1 chloroform:methanol, 2 ml of phenol (1.2 mM), 0.5 ml 2,2′-dipyridyl (2.0 mM), and 2 ml of deionised water. The 2,2′-dipyridyl was used to inhibit *ex vivo* ferrous dependant reaction, and the phenol was used as antioxidant to protect from *ex vivo* oxidation. 16 ml of 2:1 chloroform:methanol mixture were finally added to this homogenate. The sample was shaken and then centrifuged at 2000 × *g* for 10 min at 4 °C (Sigma 3K15). The chloroform layer was isolated and evaporated up to 0.5 ml final volume by bubbling with N_2. Immediately after solvent evaporation, the samples were loaded in a glass micropipet of 50 μl (Drummond, USA) and inserted in a 3 mm quartz tube. The tube was placed in the cavity of the ESR spectrometer (Brucker, ESP 380) operating on continuous waves mode at a microwave frequency of 9.71 GHz at controlled temperature (22 °C). The instrumental parameters were: microwave power of 10 mW, modulation frequency at 100 kHz with a modulation amplitude of 0.81 G, receiver gain set at 4×10^5 and scan range of 100 G with magnetic field centred at 3430 G. Each sample was scanned for up to 14 min, using the following acquisition parameters: time constant of 82 ms, conversion time 82 ms and 20 repetitions. Fig. 1B shows a typical ESR spectrum.

An estimation of free radicals production was obtained by measuring the amplitude of the central line.

2.5. Inflammation marker analysis

Quantification of Leptin, TNF-α, IGF1, IL-6, VEGF, IL-1β, IL-1 α and G-CSF were performed by using Mouse Cytokine ELISA Strip I for profiling 8 Cytokines (Signosis inc., Sunnyvale, United States) kit, according to the manufacturer's instructions. The protein standards (Mouse Standard ELISA strip) were used for control (Signosis inc., Sunnyvale, United States). The optical density of each well was measured in a microtiter plate fluorometer Mithras LB 940 at 450 nm (Berthold Technologies,

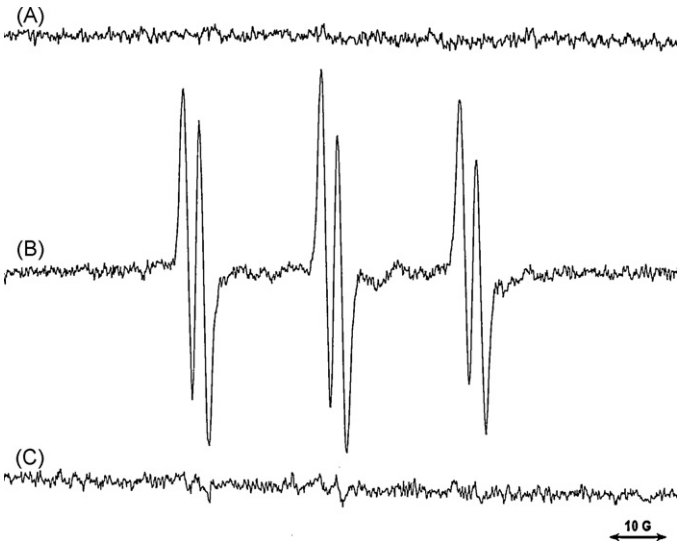

Fig. 2. *In vitro* detection of radical adducts. (A) Free radical generation in presence of DWCNTs: electron paramagnetic resonance spectra of N-tert-butyl-a-(4-pyridyl)-nitrone N'oxide (4-POBN) radical adducts following the incubation with DWCNTs. (B) Positive control: ESR spectrum of POBN/•OH adduct detected after Fenton reaction as control. (C) same as B with addition of DWCNTs.

Bad Wildbad, Germany) and processed by using the MikroWin software. All ELISA measurements were performed on serum samples only.

2.6. Microscopy and histopathology

Negative staining of nanotubes: 10 μl of nanotubes suspended in distilled water were deposed on a cooper grid for electron microscopy. These suspensions were contrasted with an aqueous solution of 2% uranyl acetate (Electron Microscopy Science, Fort Washington, Pa, USA) and observed on a transmission electron microscope JEOL 1010 at 80 kV.

Histology: Lungs from mice of control or treated groups were fixed with 3.7% formaldehyde (Sigma Aldrich, Saint Louis, Missouri, USA) in Sodium Phosphate buffer solution at a pH of 7.4. Rinsed lung were macroscopically examined with leica stereozoom 2. After paraffin embedding, 5 μm sections were cut and stained with hemalun phloxine safran (HPS) for histopathologic evaluation. For lungs injury or cellular changes and inflammation, the airways, terminal bronchioles and lungs parenchyma were examined also microscopically.

2.7. In vitro ESR spin trapping investigation

These experiments were used to investigate CNTs capacity to generate or to scavenge free radicals. The anti-radical activity was assessed by *in vitro* spin trapping experiment. Reactive oxygen species were generated immediately before ESR experiment by a Fenton reaction ($FeSO_4$, 0.1 mM and H_2O_2, 0.1 mM). The formation of short-life radical species (•OH) was evidenced by addition of water soluble spin trapping agent (4-POBN). These reactions were performed in an Eppendorf tube where 100 μl of $FeSO_4$ was mixed with 100 μl of 4-POBN spin trap and with 10 μl CNTs solution (25 mg/ml). The trigger of reaction was induced by adding 100 μl of H_2O_2 to the sample. Reference samples were prepared by replacing CNTs by distilled water.

The samples were transferred in 20 μl Pyrex capillary tubes and placed in a 3 mm diameter quartz holder.

The spectra were acquired using the continuous wave mode with a ESP 380 (Brucker) The instrumental parameter were: microwave power of 10 mW, modulation frequency at 100 kHz with a modulation amplitude of 0.51 G, receiver gain was 6.30×10^4 and scan range was 100 G with magnetic field centred at 3430 G. Each sample was scanned 3 times at controlled temperature 295 K, with the following acquisition parameters: Time constant 20.48 ms, conversion time 20.48 ms. All the experiments were performed 3 times. Fig. 2B shows typical ESR spectra of the control groups with the 4-POBN spin trap.

2.8. Statistics

All results are presented as mean ± SEM. Experiments were realized ten times. The different exposure conditions were randomized. Statistical comparisons were achieved using non-parametric tests. Significance was determined using Mann–Whitney test for unpaired data.

3. Results

3.1. Microscopy histopathology

Nanotubes: Nanotubes are present as long linear structures with a median outer diameter of 2 nm when individual and a length of several micrometers. These structures are flexible and regular, without segmentation or ramifications. At a higher level, they are self-organized either in ropelike structures with a diameter up to 80 nm, or in globular masses (Fig. 3A and B).

Macroscopy: Dense material as well as an inflammatory area can be detected in the lungs of 24 h treated mice, at a central localisation, near bronchioles. Peripherical parenchyma appears clear (Fig. 3C).

Histology: Small clusters of dense materiel are noted in the lumen of lobar bronchus, 6 h after instillation at the proximity of apex of epithelial cells (Fig. 3D). Large clusters are especially noted in bronchioles and alveoli 24 h after instillation (Fig. 3E), when after 48 h only a few material can be observed in the lumen of bronchus.

Macrophages are more frequently seen in DWCNTs groups than in control tissue, but never at an extensive level (Fig. 3F).

Compared to control lungs, a thickening of alveolar walls can be noted in treated lungs. Focally noted at 6 h after instillation, this aspect is seen in the major part of the tissue at 24 and 48 h (Fig. 3G and H).

3.2. In vitro assessment of ROS generation or scavenging activity by CNTs

The potential of CNTs to release free radicals in aqueous suspension was monitored by ESR spectroscopy with 4-POBN as trapping agent. The generation of •OH in the presence of H_2O_2 mimics the contact of particles with physiological fluids during their phagocytosis by alveolar macrophages and recruited granulocytes (Fenoglio et al., 2006). The yield of •OH was followed by measuring the intensity of the spectrum of the 4-POBN/OH adducts. As shown on Fig. 2A nanotubes are not able to produce any delectable radicals when they are put in presence of H_2O_2 solution. Fig. 2B shows the typical 6 line spectra obtained by the positive control Fenton Reaction. The reaction was repeated in the presence of 10 μl (25 mg/ml) CNTs solution. In this case the signal of the 4-POBN/OH adducts was almost completely suppressed (Fig. 2C).

3.3. In vivo ROS production

Six hours after intranasal saline administration, three-lines ESR spectra could be detected in sample of saline instilled mice (Fig. 1A). This signal was not attributed to a specific POBN/Radical adduct, but is probably resulting from interaction of many different radical species (•OH, O_2, CH_3, Lipid derivate radical) naturally present in the lungs. The administration of bleomycin as positive control leads to the same ESR spectrum with the same splitting constants but with a significantly enhanced signal (Fig. 1B), while 24 h after CNTs instillation the spectra is significantly lower than the control (Fig. 1C).

The comparison of the ROS production between the control group and the different DWCNTs groups are shown in Fig. 4. For each group the ROS production was assessed by measuring the intensity of the middle line of each spectrum, and was expressed in arbitrary units. For the whole CNTs exposed group, CNTs instillation induces a decrease in the ROS production. At the earliest time (6 h), this decrease is 19% lower than control but does not appear as statistically significant. This drop in the oxidative stress production reaches significance ($p < 0.01$) 24 h after instillation with a decrease of 54% of the ESR signal and remain unchanged 48 h after with 55% less of ROS than control.

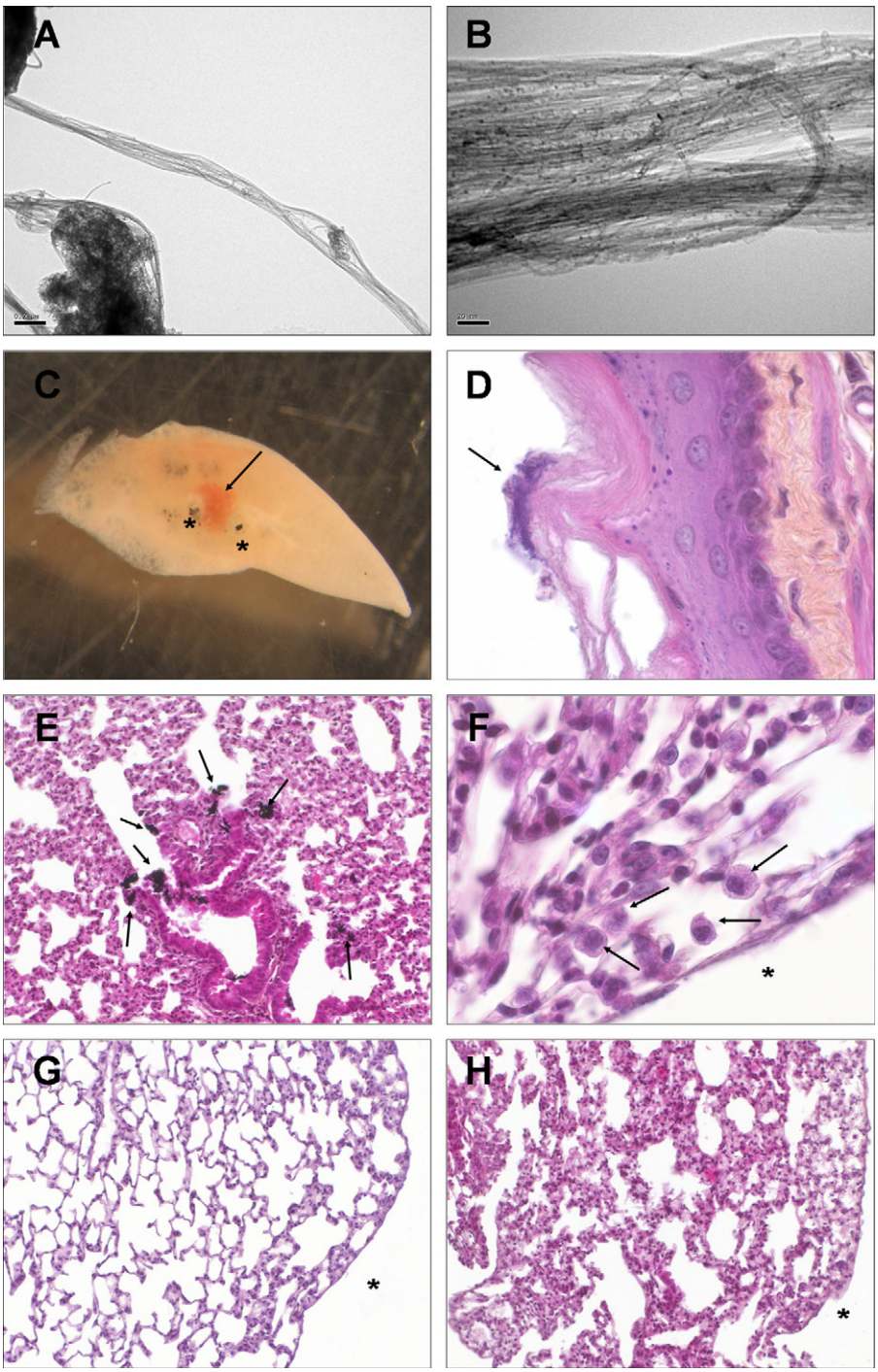

Fig. 3. (A) Electron microscopical image of DWCNTs, in linear structures and globular masses. Magnification 50,000× scale 0.2 μm. (B) Higher magnification of DWCNTs showing their ropelike aspect. Magnification 500,000× scale 20 nm. (C) Microscopical aspect of lungs, 24 h after instillation. Dense clusters of DWCNTs (*) and inflammation area (arrow) can be noticed in central parenchyma, near bronchioles. (D) Lumen of lobar bronchus 6 h after instillation of DWCNTs. Cluster of dense material deposed in the mucus (arrows). Magnification 200×. (E) DWCNTs deposit in the lumen of terminating bronchioles and in the neighbouring pulmonary alveoli (arrows), 24 h after instillation. Magnification 200×. (F) Lungs 48 h after instillation. Macrophages can be noted in the alveoli (arrow). Magnification 1000×. Delimiting pleura (*). (G) Control lungs in peripheral lobar area. (*) shows the delimiting pleura. Magnification 200×. (H) Peripheral lobar area of lung, 24 h after instillation, showing the thickening of alveolar walls and the diminution of alveolar space. (*) shows the delimiting pleura. Magnification 200×.

3.4. *Inflammatory response*

The inflammatory response was assessed by measuring the cytokine concentration in plasma. Our attention was focused on TNF-α, IL-1α, IL-1β, IL-6, IGF-1, Leptin, G-CSF, and VEGF. Despite the lack of increase in ROS production in CNTs groups, a significant systematic inflammatory response was evidenced as shown on Fig. 5. Whatever the time after CNTs administration, leptin concentration is significantly higher (control: 3954 ± 332 pg/ml, 6 h group 5755 ± 385 pg/ml, 24 h group 5116 ± 323 pg/ml and 48 h group 6381 ± 856 pg/ml). The concentration of the other cytokine is not different except IL-6, which reaches significance at 48 h (517 ± 36 pg/ml for control, 709 ± 56 pg/ml for 48 h group).

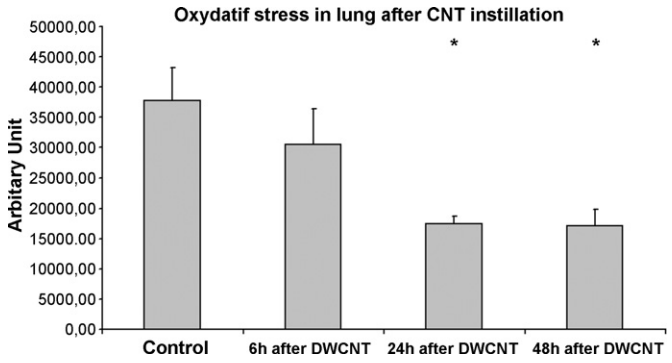

Fig. 4. Mean free radical production after DWCNTs intranasal instillation. Each value was expressed as relative value to the control group. For each group value was the mean of 10 measure ± SD. The statistically significance was indicated by * ($p < 0.01$) (Mann–Whitney *U*-test).

4. Discussion

Pulmonary toxicity of CNTs bares a very specific place in term of public health with the wide spreading of these new materials. With their morphology similar to asbestos fibres, the assessment of the respiratory toxicity focuses the attention of many scientists.

In vivo studies dealing with CNT pulmonary toxicity are currently discussing about the best protocol to be used to administrate CNTs. While inhalation is the most physiological method, the impossibility to assess the administrated quantity of CNTs, leads this protocol not to be usable for toxicological studies (Maynard and Aitken, 2007). Intranasal or intra-tracheal instillation is the most common administration method. However due to their hydrophobic properties, CNTs are known to create large size agglomerate when directly dispersed in suspension in saline. These aggregates could lead to an overestimation of the acute CNT toxicity. Warheit et al. (2004) demonstrated that intranasal instillation of 5 mg/kg of SWCNTs in saline leads to a high mortality of rats (15%), nevertheless this mortality was not due to inherent toxicity of SWCNTs but was due to the impact of agglomerates that jammed the major airways in the rat. The most common way to overcome this effect was the use of Bovine Serum Albumin (BSA) as dispersing agent in CNTs suspension. In that way, agglomerates were not discarded, while BSA improved the formation of small and breathable CNTs

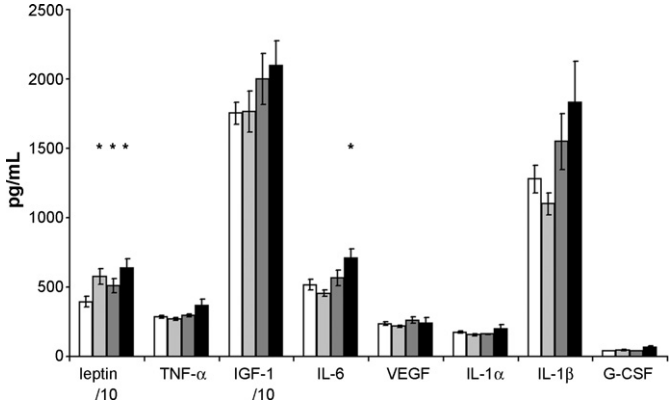

Fig. 5. Concentration of the cytokines Leptin, TNF-α, IGF1, IL-6, VEGF, IL-1β, IL-1 α and G-CSF were determined in serum of mice by the ELISA technique. The concentration in pg/ml of cytokines in the serum were determined in control group (white), at 6 (light grey), 24 (dark grey) and 48 (black) hours after administration of DWCNTs. Leptin and IGF-1 concentration were divided per 10 for the clarity of the figure. Data are shown as means ± SEM for $n = 8$ and the statistically significant differences are indicated by * ($p < 0.05$) (Mann–Whitney *U*-test).

aggregate (<10 μm) (Elgrabli et al., 2009). However some authors pointed out those proteins such as BSA could also modulate the CNT-induced toxicity. In human blood serum CNT-Albumin interaction leads to a CNT-Albumin complex which could bind with class A Scavenger receptor (Dutta et al., 2007; Elgrabli et al., 2008): earlier work indicated clearly that human albumin adsorbs on DWCNTs (Salvador-Morales et al., 2006). These receptors modulate organism immune response and clearance capacity of CNTs (Dutta et al., 2007). Using BSA as dispersing agent could produce a CNT-Albumin complex and activate the class A receptors. This led to avoid the use of BSA in the present study, by sonicating the aggregates to obtain their dispersion, even if the resulting structures could be bigger than those produced following the BSA method: as a first result, no animal death was observed, and no modulation of immune response could be attributed to the administration protocol. The histological observation confirmed the breathable size of particle, and the homogeneity of size repartition. Time evolution allowed a deeper penetration of CNTs in the lungs structure, starting with a main presence in the bronchus after 6 h, to an intra-alveolar location at 24 and 48 h. As *in vitro* model (Debouzy et al., 2010), no crossing of the cell membrane could be observed.

Twenty-four hours after CNTs instillation a thickening of alveolar walls and a diminution of alveolar space could be observed. According to Wang et al results (Wang et al., 2010), this feature would be attributed to the early stimulation of collagen production by lung interstitium fibroblast after dispersed CTNs exposure. Besides, larges agglomerates induce an inflammatory reaction. Our results are in accordance with the persistence of dispersed CNTs and agglomerates in the instillation assay.

An increase in alveolar macrophages was clearly noted after 24 h. This observation is in full agreement with many previous works reporting inflammatory reactions with granuloma formation, macrophage migration and local pro-inflammation cytokine (Inoue et al., 2010; Mangum et al., 2006; Muller et al., 2005; Shvedova et al., 2005; Warheit, 2006).

From this it was interesting to address the general repercussion of this local inflammation. Systemic inflammatory reaction was confirmed by Elisa inflammation test.

Besides, the concentration of leptin, a marker of the lung inflammation (Broekhuizen et al., 2005b; Shore et al., 2005; Tas et al., 2005), was found significantly higher in all CNT groups. Among the others cytokines measured, only IL6 levels appeared significantly increased at 48 h. These results are consistent with the existence of chronic reactions related to the persistence of CNTs in the lung (48 h). Another recent paper also suggested that the inflammatory response and DNA damage strongly depend on the size and shape of CNT (Yamashita et al., 2010). The major effects appeared for thick multiwalled CNTs (length 5–15 μm, diameter 20–60 nm) while few effects were shown for thin single walled CNTs (length 5–15, diameter < 2 nm). The use in our study of thin DWCNTs (length 10 μm, diameter 3.2 nm) should lead to a slight inflammation reaction. This hypothesis is not in agreement with our results. This difference would probably be attributed to the lack of use of dispersing agent for the DWCNT administration by opposition with Yamashita results. As previously described, DWCNT created bundles and aggregates of significantly bigger size and could be compared to thick multiwalled CNTs.

Conversely, no significant increase of TNF-α was measured in plasma despite the inflammation process. These limited changes in plasma cytokines is not surprising since cytokines produced in the lung were then diluted by the entire blood volume. Other works also noticed the absence of any significant increase of TNF-α after nanoparticles exposure on triple co-cultured cells (Muller et al., 2010). The author firstly suggested that this effect could be the consequence of cytokine binding on particles; however the same absence of effect was observed with 3 totally different particles

types thus leading the author to consider this hypothesis as unrealistic.

It is well established that inflammation increases the ROS production (Babior, 1978; Martins Chaves et al., 2000; Roessner et al., 2008); moreover, some publications consider that CNTs toxicity in directly related with an increase in ROS production (Manna et al., 2005; Tan et al., 2009). Inoues study (Inoue et al., 2010) had shown that SWCNTs intratracheally administrated, exacerbated allergen-related airway inflammation, concomitant with the increased at the lung level of many proinflammatory cytokines as IL-1β, IL6 and potentiated formation/activity of oxidative stress. Such a ROS production was not found in the present work: the discrepancy could be related to the purity of the CNTs used in this study, i.e. bioavailable metal-free structures. Hence ROS production has recently been reported when cells were stimulated with unpurified CNTs (Pulskamp et al., 2007; Shvedova et al., 2003), which means containing high amounts of metallic ions coming from the synthesis process. Inoue et al (Inoue et al., 2010) had observed a correlation between the remaining metal concentration in CNTs and the evaluated oxidative stress. From this results one could considered that the increase of the oxidative stress could be attributed to the used of CNTs with a very high concentration of remaining metal (from 7 to 23%, w/w).

Our present *in vitro* results confirmed Fengolio results (Fenoglio et al., 2006): this author suggested that similarly to fullerenes, ROS may be "grafted" at the surface of CNTs via radical addition for the carbon framework. Such mechanisms are frequently used for polymer grafting or functionalization of nanotubes. The scavenging properties of CNTs have also been attributed to their high electron affinity, similar to that of C_{60}. From this, one can suggest that *in vivo*, CNTs truly induce an inflammation reaction, involving macrophage recruitment. However, even if macrophages release ROS in their vicinity, CNTs trap the radicals thus resulting in a decrease in the local oxidative stress.

Moreover, according to Muller's works (Muller et al., 2010) most of the studies, performed on single culture cells overestimate the oxidative stress after nanoparticles exposure. This author showed a significant decrease of the oxidative stress value between a triple cell co-cultured model and the theoretical value obtained with 3 monocultures. Also a variation in TNF-α and IL 8 release was observed. Such results suggested that the interplay of different lung cell types seems to substantially modulate the oxidative stress and the inflammatory response after nanoparticles exposure. The lack of increase of ROS production in our *in vivo* experiment is consistent with this study.

This effect decreases the tissue damages linked to the ROS reactivity (i.e. lipid peroxydation, protein recombination or DNA damages) and could be associated to a lower toxicity. Nevertheless it should be emphasis that ROS production during the inflammation is a way of bacterial elimination and control of the infections. Finally, beside an apparent reduced toxicity, CNTs could weaken the natural defenses against bacterial or virus and so facilitated theirs development during a concomitant infection.

In conclusion, the present study shows that purified DWCNTs induce an inflammatory reaction in lungs. However, the ROS scavenger capability of CNTs limits the resulting oxidative stress. Other consequences are, on the one hand a reduced toxicity of CNTs, and on the other hand possible adverse effects of CNTs when a lung infection is present. The *in vivo* effects of unpurified CNTs should also be investigated. These investigations are now in progress.

Conflict of interest

The authors declare that there are no conflicts of interest.

References

Babior, B.M., 1978. Oxygen-dependent microbial killing by phagocytes (second of two parts). N. Engl. J. Med. 298, 721–725.

Broekhuizen, R., Vernooy, J.H., Schols, A.M., Dentener, M.A., Wouters, E.F., 2005a. Leptin as local inflammatory marker in COPD. Respir. Med. 99, 70–74.

Broekhuizen, R., Vernooy, J.H.J., Schols, A.M.W.J., Dentener, M.A., Wouters, E.F.M., 2005b. Leptin as local inflammatory marker in COPD. Respir. Med. 99, 70–74.

Brown, D.M., Beswick, P.H., Bell, K.S., Donaldson, K., 2000. Depletion of glutathione and ascorbate in lung lining fluid by respirable fibres. Ann. Occup. Hyg. 44, 101–108.

Castranova, V., 2004. Signaling pathways controlling the production of inflammatory mediators in response to crystalline silica exposure: role of reactive oxygen/nitrogen species. Free Radical Biol. Med. 37, 916–925.

Crouzier, D., Perrin, A., Torres, G., Dabouis, V., Debouzy, J.C., 2009. Pulsed electromagnetic field at 9. 71 GHz increase free radical production in yeast (Saccharomyces cerevisiae). Pathol. Biol. (Paris) 57, 245–251.

Debouzy, J.C., Crouzier, D., Flahaut, E., 2010. Hydrophobic double walled carbon nanotubes interaction with phopholipidic model membranes: a 1H-, 2H-, 31P-NMR and ESR study. Environ. Toxicol. Pharmacol., in press.

Dutta, D., Sundaram, S.K., Teeguarden, J.G., Riley, B.J., Fifield, L.S., Jacobs, J.M., Addleman, S.R., Kaysen, G.A., Moudgil, B.M., Weber, T.J., 2007. Adsorbed proteins influence the biological activity and molecular targeting of nanomaterials. Toxicol. Sci. 100, 303–315.

Elgrabli, D., Abella-Gallart, S., Robidel, F., Rogerieux, F., Boczkowski, J., Lacroix, G., 2008. Induction of apoptosis and absence of inflammation in rat lung after intratracheal instillation of multiwalled carbon nanotubes. Toxicology 253, 131–136.

Elgrabli, D., Abella-Gallart, S., Aguerre-Chariol, O., Robidel, F., Rogerieux, F., Boczkowski, J., Lacroix, G., 2009. Effect of BSA on carbon nanotube dispersion for in vivo and in vitro studies. Nanotoxicology 1, 266–278.

Fenoglio, I., Martra, G., Coluccia, S., Fubini, B., 2000. Possible role of ascorbic acid in the oxidative damage induced by inhaled crystalline silica particles. Chem. Res. Toxicol. 13, 971–975.

Fenoglio, I., Tomatis, M., Lison, D., Muller, J., Fonseca, A., Nagy, J.B., Fubini, B., 2006. Reactivity of carbon nanotubes: free radical generation or scavenging activity? Free Radical Biol. Med. 40, 1227–1233.

Flahaut, E., Durrieu, M.C., Remy-Zolghadri, M., Bareille, R., Baquey, C., 2006. Investigation of the cytotoxicity of CCVD carbon nanotubes towards human umbilical vein endothelial cells. Carbon 44, 1093–1099.

Inoue, K.-i., Yanagisawa, R., Koike, E., Nishikawa, M., Takano, H., 2010. Repeated pulmonary exposure to single-walled carbon nanotubes exacerbates allergic inflammation of the airway: possible role of oxidative stress. Free Radical Biol. Med. 48, 924–934.

Kamp, D.W., Graceffa, P., Pryor, W.A., Weitzman, S.A., 1992. The role of free radicals in asbestos-induced diseases. Free Radical Biol. Med. 12, 293–315.

Kane, A.B., 1996. Mechanisms of mineral fibre carcinogenesis. IARC Sci. Publ., 11–34.

Karapanagiotou, E.M., Tsochatzis, E.A., Dilana, K.D., Tourkantonis, I., Gratsias, I., Syrigos, K.N., 2008. The significance of leptin, adiponectin, and resistin serum levels in non-small cell lung cancer (NSCLC). Lung Cancer 61, 391–397.

Lam, C.W., James, J.T., McCluskey, R., Hunter, R.L., 2004. Pulmonary toxicity of single-wall carbon nanotubes in mice 7 and 90 days after intratracheal instillation. Toxicol. Sci. 77, 126–134.

Mangum, J.B., Turpin, E.A., Antao-Menezes, A., Cesta, M.F., Bermudez, E., Bonner, J.C., 2006. Single-walled carbon nanotube (SWCNT)-induced interstitial fibrosis in the lungs of rats is associated with increased levels of PDGF mRNA and the formation of unique intercellular carbon structures that bridge alveolar macrophages in situ. Part Fibre Toxicol. 3, 15.

Manna, S.K., Sarkar, S., Barr, J., Wise, K., Barrera, E.V., Jejelowo, O., Rice-Ficht, A.C., Ramesh, G.T., 2005. Single-walled carbon nanotube induces oxidative stress and activates nuclear transcription factor-kappaB in human keratinocytes. Nano Lett. 5, 1676–1684.

Martins Chaves, M., Rocha-Vieira, E., Pereira dos Reis, A., de Lima e Silva, R., Gerzstein, N.C., Nogueira-Machado, J.A., 2000. Increase of reactive oxygen (ROS) and nitrogen (RNS) species generated by phagocyting granulocytes related to age. Mech. Ageing Dev. 119, 1–8.

Maynard, A.D., Aitken, R.J., 2007. Assessing exposure to airborne nanomaterials: current abilities and future requirements. Nanotoxicology 1, 26–41.

Muller, J., Huaux, F., Moreau, N., Misson, P., Heilier, J.-F., Delos, M., Arras, M., Fonseca, A., Nagy, J.B., Lison, D., 2005. Respiratory toxicity of multi-wall carbon nanotubes. Toxicol. Appl. Pharmacol. 207, 221–231.

Muller, L., Riediker, M., Wick, P., Mohr, M., Gehr, P., Rothen-Rutishauser, B., 2010. Oxidative stress and inflammation response after nanoparticle exposure: differences between human lung cell monocultures and an advanced three-dimensional model of the human epithelial airways. J. R. Soc. Interface 7 (Suppl. 1), S27–S40.

Park, E.-J., Cho, W.-S., Jeong, J., Yi, J., Choi, K., Park, K., 2009. Pro-inflammatory and potential allergic responses resulting from B cell activation in mice treated with multi-walled carbon nanotubes by intratracheal instillation. Toxicology 259, 113–121.

Peigney, A., Laurent, C., Flahaut, E., Bacsa, R.R., Rousset, A., 2001. Specific surface area of carbon nanotubes and bundles of carbon nanotubes. Carbon 39, 507–514.

Poland, C.A., Duffin, R., Kinloch, I., Maynard, A., Wallace, W.A.H., Seaton, A., Stone, V., Brown, S., MacNee, W., Donaldson, K., 2008. Carbon nanotubes introduced into the abdominal cavity of mice show asbestos-like pathogenicity in a pilot study. Nat. Nano 3, 423–428.

Pulskamp, K., Diabaté, S., Krug, H.F., 2007. Carbon nanotubes show no sign of acute toxicity but induce intracellular reactive oxygen species in dependence on contaminants. Toxicol. Lett. 168, 58–74.
Roessner, A., Kuester, D., Malfertheiner, P., Schneider-Stock, R., 2008. Oxidative stress in ulcerative colitis-associated carcinogenesis. Pathol.: Res. Pract. 204, 511–524.
Salvador-Morales, C., Flahaut, E., Sim, E., Sloan, J., Green, M.L.H., Sim, R.B., 2006. Complement activation and protein adsorption by carbon nanotubes. Mol. Immunol. 43, 193–201.
Sato, K., Tashiro, Y., Chibana, S., Yamashita, A., Karakawa, T., Kohrogi, H., 2008. Role of lipid-derived free radical in bleomycin-induced lung injury in mice: availability for ESR spin trap method with organic phase extraction. Biol. Pharm. Bull. 31, 1855–1859.
Shore, S.A., Schwartzman, I.N., Mellema, M.S., Flynt, L., Imrich, A., Johnston, R.A., 2005. Effect of leptin on allergic airway responses in mice. J. Allergy Clin. Immunol. 115, 103–109.
Shvedova, A.A., Castranova, V., Kisin, E.R., Schwegler-Berry, D., Murray, A.R., Gandelsman, V.Z., Maynard, A., Baron, P., 2003. Exposure to carbon nanotube material: assessment of nanotube cytotoxicity using human keratinocyte cells. J. Toxicol. Environ. Health A 66, 1909–1926.
Shvedova, A.A., Kisin, E.R., Mercer, R., Murray, A.R., Johnson, V.J., Potapovich, A.I., Tyurina, Y.Y., Gorelik, O., Arepalli, S., Schwegler-Berry, D., Hubbs, A.F., Antonini, J., Evans, D.E., Ku, B.K., Ramsey, D., Maynard, A., Kagan, V.E., Castranova, V., Baron, P., 2005. Unusual inflammatory and fibrogenic pulmonary responses to single-walled carbon nanotubes in mice. Am. J. Physiol. Lung Cell Mol. Physiol. 289, L698–708.
Stadtman, E.R., 1990. Covalent modification reactions are marking steps in protein turnover. Biochemistry 29, 6323–6331.
Tan, X.-m., Lin, C., Fugetsu, B., 2009. Studies on toxicity of multi-walled carbon nanotubes on suspension rice cells. Carbon 47, 3479–3487.
Tas, F., Duranyildiz, D., Argon, A., Oguz, H., Camlica, H., Yasasever, V., Topuz, E., 2005. Serum levels of leptin and proinflammatory cytokines in advanced-stage non-small cell lung cancer. Med. Oncol. 22, 353–358.
Wang, L., Mercer, R.R., Rojanasakul, Y., Qiu, A., Lu, Y., Scabilloni, J.F., Wu, N., Castranova, V., 2010. Direct fibrogenic effects of dispersed single-walled carbon nanotubes on human lung fibroblasts. J. Toxicol. Environ. Health A 73, 410–422.
Warheit, D.B., 2006. What is currently known about the health risks related to carbon nanotube exposures? Carbon 44, 1064–1069.
Warheit, D.B., Laurence, B.R., Reed, K.L., Roach, D.H., Reynolds, G.A., Webb, T.R., 2004. Comparative pulmonary toxicity assessment of single-wall carbon nanotubes in rats. Toxicol. Sci. 77, 117–125.
Yamashita, K., Yoshioka, Y., Higashisaka, K., Morishita, Y., Yoshida, T., Fujimura, M., Kayamuro, H., Nabeshi, H., Yamashita, T., Nagano, K., Abe, Y., Kamada, H., Kawai, Y., Mayumi, T., Yoshikawa, T., Itoh, N., Tsunoda, S.I., Tsutsumi, Y., 2010. Carbon nanotubes elicit DNA damage and inflammatory response relative to their size and shape. Inflammation.